Human Molecular Genetics, 2012, Vol. 21, No. 26 ***5528–5538***
doi:10.1093/hmg/dds408
Advance Access published on October 1, 2012

The ciliopathy disease protein NPHP9 promotes nuclear delivery and activation of the oncogenic transcriptional regulator TAZ

Sandra Habbig[1,2,†], Malte P. Bartram[1,†], Josef G. Sägmüller[1], Anabel Griessmann[1], Mareike Franke[1], Roman-Ulrich Müller[1,5], Ricarda Schwarz[1], Martin Hoehne[1,3], Carsten Bergmann[6,7,8], Claudia Tessmer[9], H. Christian Reinhardt[4,5], Volker Burst[1], Thomas Benzing[1,3,5], and Bernhard Schermer[1,3,5,*]

[1]Department II of Internal Medicine and Center for Molecular Medicine Cologne, [2]Department of Pediatrics, [3]Systems Biology of Ageing Cologne (Sybacol) and [4]Department I of Internal Medicine, University of Cologne, 50937 Cologne, Germany, [5]Cologne Excellence Cluster on Cellular Stress Responses in Aging-Associated Diseases, University of Cologne, 50674 Cologne, Germany, [6]Center for Human Genetics, Bioscientia, Ingelheim, Germany, [7]Department of Human Genetics, RWTH Aachen University, Germany, [8]Center for Clinical Research, Freiburg University, Germany and [9]Monoclonal Antibody Facility, German Cancer Research Center, Heidelberg, Germany

Received August 5, 2012; Revised and Accepted September 24, 2012

Nephronophthisis (NPH) is a genetically heterogenous kidney disease and represents the most common genetic cause for end-stage renal disease in children. It is caused by the mutation of genes encoding for the nephrocystin proteins (NPHPs) which localize to primary cilia or centrosomes, classifying this disease as a 'ciliopathy'. Recently, it has been shown that NPHP4 acts as a potent negative regulator of mammalian Hippo signalling by interacting with the Lats protein kinase and controlling the phosphorylation of the oncogenic transcriptional activator TAZ. Here, we demonstrate that NPHP9, another NPH family member, also controls TAZ activity by a distinct mechanism. NPHP9, which is also called NEK8, directly interacted with TAZ and induced nuclear translocation of the TAZ/NPHP9 protein complex. Binding of NPHP9 to TAZ was enhanced in a TAZ mutant that lost its ability to bind 14-3-3, suggesting that 14-3-3 and NPHP9 may compete for TAZ binding, with 14-3-3 favouring cytoplasmic retention and NPHP9 mediating nuclear delivery. Consistently, co-expression of NPHP4, which inhibits TAZ phosphorylation at the 14-3-3 binding site through the inhibition of Lats kinase activity, induced efficient nuclear delivery of the TAZ/NPHP9 protein pair. Consistent with a role for TAZ in controlling proliferation and tumorigenesis, the downregulation of NPHP9 inhibited the TAZ-dependent proliferation of hippo-responsive normal epithelial and also breast cancer cells. As NPHP9 has been shown to be upregulated in breast cancer, these data do not only support a critical role for TAZ/hippo signalling in the pathogenesis of NPH but may also imply a possible role for NPHP9 in TAZ-mediated tumorigenesis.

INTRODUCTION

Nephronophthisis (NPH) is a genetically heterogeneous cystic kidney disease and a leading genetic cause for endstage renal disease in children and young adults. Mutations in 12 causative genes (*NPHP1–12*; NPHP, nephrocystin protein) have been described (1,2). Interestingly, the vast majority of the NPH proteins localizes to the base of primary cilia, sensory organelles

*To whom correspondence should be addressed at: Department II of Internal Medicine, University of Cologne, Kerpener Str. 62, 50937 Cologne, Germany. Tel: +49 22147889030; Fax: +49 22147889041; Email: bernhard.schermer@uk-koeln.de
†These authors contributed equally to this work.

that are integrating cues received from the microenvironment (2,3). Despite the growing knowledge of the underlying genetics and definition of NPH as a ciliopathy, the function of these proteins has remained unclear. Several NPHP-associated disease mechanisms have been proposed in literature previously, including ciliary signalling such as Wnt and Sonic hedgehog (Shh) as well as the regulation of planar cell polarity (4). Recently, we could show that NPHP4 inhibits the hippo signalling pathway and suggested that deregulated hippo signalling may contribute to the pathogenesis of NPH. NPHP4 exerted pro-proliferative effects through inhibiting hippo signalling. Accordingly, de-repressed hippo signalling in the case of loss of NPHP4 was thought to decrease the proliferative potential, which may contribute to small, degenerative kidneys—a phenotypic hallmark in NPH (5). However, this finding had not been extended to other NPH proteins.

The hippo pathway was first described in *Drosophila melanogaster* (6). The core complex consists of a classical kinase cascade: activation increases the phosphorylation of the kinase MST1/2 (Mammalian Sterile 20-Like Kinase), which in turn results in the phosphorylation of LATS1/2 (Large Tumour Suppressor 1/2) that ultimately mediates the phosphorylation and thereby cytoplasmic retention and inactivation of the transcriptional co-activators TAZ (transcriptional co-activator with PDZ-binding motif) and YAP (Yes-associated protein). Recently, the hippo pathway has gained increasing attention since it was shown that hippo signalling controls cell proliferation, organ size determination and tumorigenesis (7–9). Moreover, the effector proteins YAP and TAZ have been shown to act as oncogenes in a number of different types of cancer. In particular, TAZ has been described to be involved in non-small-cell lung cancer (10), and elevated expression levels of TAZ were found in breast cancer (11,12) and in breast cancer stem cells (13). Interestingly, loss of TAZ in two different mouse models resulted in kidney phenotypes reminiscent of the pathology observed in human NPH (14,15).

Nek8 (Nima-related Kinase 8) is a member of the NEK family of kinases and the encoding gene has recently been identified as *NPHP9* (16). Mutations in *NPHP9* are also responsible for the cystic kidney disease observed in *jck* mutant mice (17) (*jck* is another NPHP9/NEK8 alias). Moreover, elevated expression levels of NPHP9 have been found in breast cancer (18). These findings prompted us to study the role of NPHP9 in hippo signalling. Here, we show that NPHP9 interacts with TAZ, thereby enhancing TAZ/TEAD-dependent transcription, whereas three disease-causing mutations in NPHP9 abrogated the effect on TAZ/TEAD activity. When analysing the role of NPHP4 in this context, we found that NPHP4 enhances the level of nuclear NPHP9, thereby promoting the TAZ–NPHP9 interaction. Taken together, this study clearly strengthens the interplay between *NPHP* genes and the hippo signalling pathway.

RESULTS

NPHP9 promotes signalling through the transcriptional co-activator TAZ

The transcriptional co-activator TAZ executes most of its activity through transcription factors of the TEAD family. TAZ is inhibited through active hippo signalling. To analyse whether NPHP9 modulates the activity of the hippo signalling pathway and its downstream effector TAZ, we performed luciferase-based reporter assays using a TEAD reporter system. The expression of TAZ induced marked upregulation of TEAD luciferase activity, which was significantly enhanced in the presence of NPHP9 (Fig. 1A). In addition, we tested NPHP5 and NPHP8, since these NPHP proteins had been implicated with cancer previously (19,20). Whereas NPHP5 did not affect TAZ/TEAD activity, NPHP8 inhibited TAZ-dependent TEAD activation (Supplementary Material, Fig. S1), consistent with a previous report on NPHP8 as a potential tumour suppressor in liver cancer (19). We then analysed whether the kinase domain of NPHP9 is required for its function on TAZ/TEAD activation. Interestingly, a kinase-dead mutant carrying a point mutation in the ATP binding pocket (K33M) similarly augmented TAZ activity as the wild-type protein (Fig. 1B), indicating that NPHP9 exerts its effect on TAZ/TEAD independent of its kinase domain. We next investigated whether patient mutations that are known causes of NPH were affecting the NPHP9-dependent TAZ control. To date, only three distinct point mutations, L330F, H425Y and A497P, have been described (16), none of which affects kinase activity (21). Interestingly, all three amino acid changes abrogated the effect of NPHP9 on TAZ activity, underscoring the clinical relevance of TAZ control through NPHP9 (Fig. 1C). Since NPHP4, another NPH disease protein, has been demonstrated to affect TAZ/TEAD activity in a similar way (5), we tested whether NPHP4 and NPHP9 would co-operate to regulate TAZ/TEAD activity. Both proteins appeared to interact in one complex (Supplementary Material, Fig. S2). We decreased the relative levels of transfected NPHP9 and NPHP4 to a dose that did not cause a significant effect on TAZ/TEAD activation (Fig. 1D). However, under these conditions, combination of both expression plasmids resulted in an enhanced stimulation of TAZ-dependent TEAD luciferase activity, indicating their interaction in this pathway. These data suggested that NPHP9 and NPHP4 co-operated to control TAZ activity.

NPHP9 translocates TAZ into the nucleus

The ability of TAZ to regulate gene transcription is tightly regulated through the phosphorylation-dependent binding of 14-3-3 proteins, resulting in 14-3-3-mediated cytoplasmic retention of TAZ (22). We therefore studied the interaction of TAZ with 14-3-3 together with TAZ phosphorylation at the serine residue-89, a major binding site of 14-3-3. Expression of NPHP9 inhibited the interaction of wild-type TAZ with 14-3-3 considerably (Fig. 2A). Consistently, NPHP9 abolished the phosphorylation of TAZ at Ser-89. Cell fractionation experiments showed a nuclear enrichment of TAZ in the presence of NPHP9, confirming these data (Fig. 2B). Interestingly, NPHP9 itself was also found predominantly in the nuclear fraction. Analysis of whole-cell lysates (WCLs) of the same experiment confirmed that NPHP9 did not influence total protein levels of TAZ (Fig. 2B, lower panel).

We next used immunofluorescence microscopy to study TAZ nuclear translocation in hippo-responsive breast

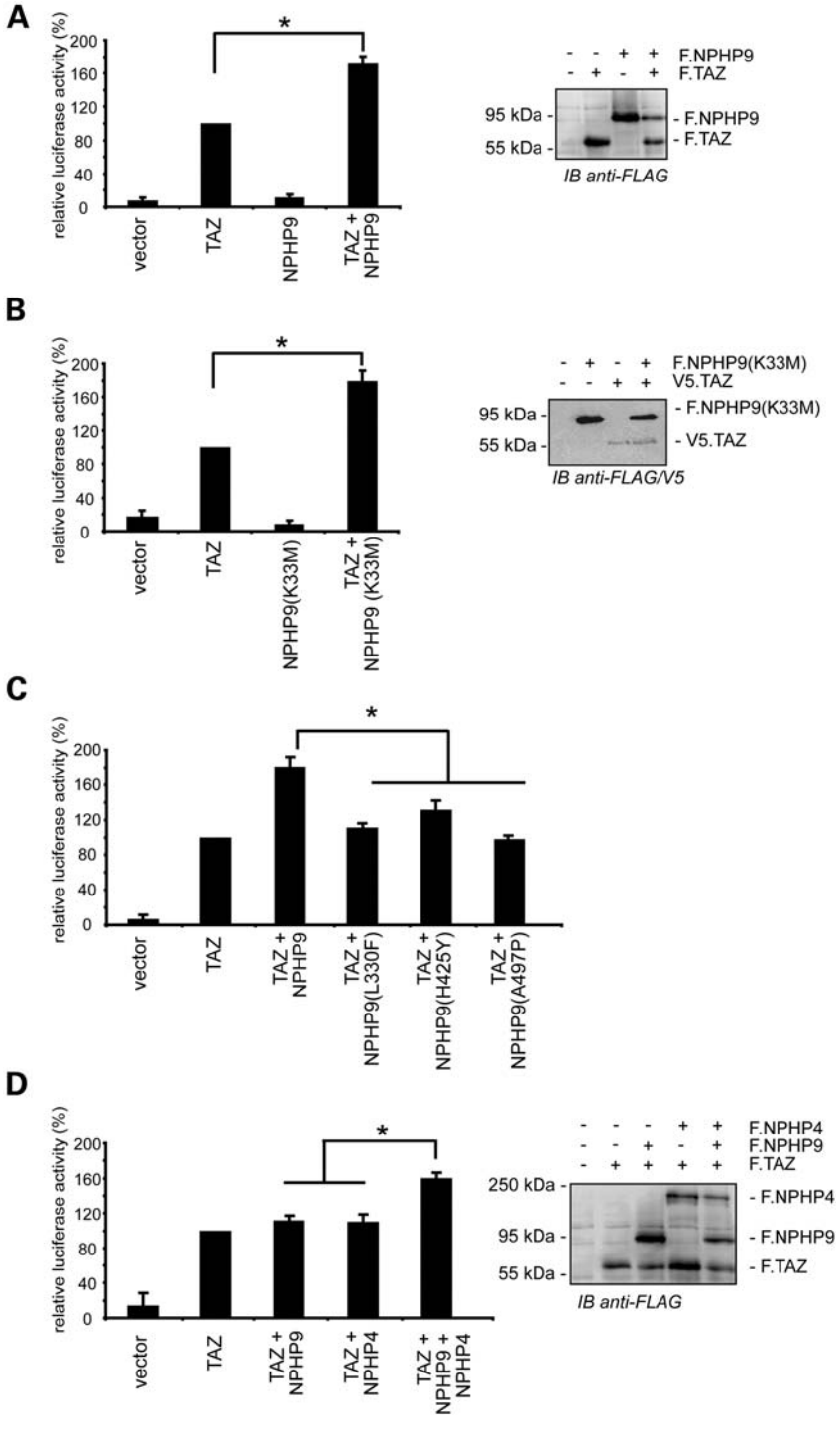

Figure 1. Wild-type but not mutant NPHP9 activates TAZ/TEAD reporter activity, and NPHP4 and NPHP9 co-operatively enhance TAZ/TEAD activity. (**A**–**D**) The indicated plasmids were co-transfected in HEK293T cells together with the luciferase reporter plasmid pGBD-Hyg-Luc, the activator plasmid pGal4-TEAD and pGL4.74 encoding the *Renilla* luciferase. Firefly luciferase activity was measured and normalized to *Renilla* luciferase activity. Signalling activity of TAZ was set to 100%. Expression of the indicated proteins was confirmed by western blot analysis. (A) Co-expression of NPHP9 significantly increased the TAZ-dependent TEAD signalling ($n = 4$; unpaired Student's *t*-test; $^{*}P < 0.05$; error bars represent SEM), whereas expression of NPHP9 alone did not affect TEAD activity. (B) The effect of NPHP9 is independent of its kinase activity. Analysis of a kinase-dead point mutant of NPHP9 (K33M) reveals a similar activation of TAZ-TEAD activation as NPHP9 wild-type ($n = 5$; unpaired Student's *t*-test; $^{*}P < 0.05$; error bars represent SEM). (C) Analysis of the three currently known patient point mutations of NPHP9 shows that these plasmids fail to activate the TAZ/TEAD reporter in comparison with NPHP9 wild-type ($n = 4$; unpaired Student's *t*-test; $^{*}P < 0.05$; error bars represent SEM). (D) After titrating down the relative DNA level to a condition in which NPHP9 and NPHP4 have no activating effect on TAZ any more, the co-expression of both proteins significantly increases the TAZ-dependent signalling ($n = 5$; unpaired Student's *t*-test; $^{*}P < 0.05$; error bars represent SEM).

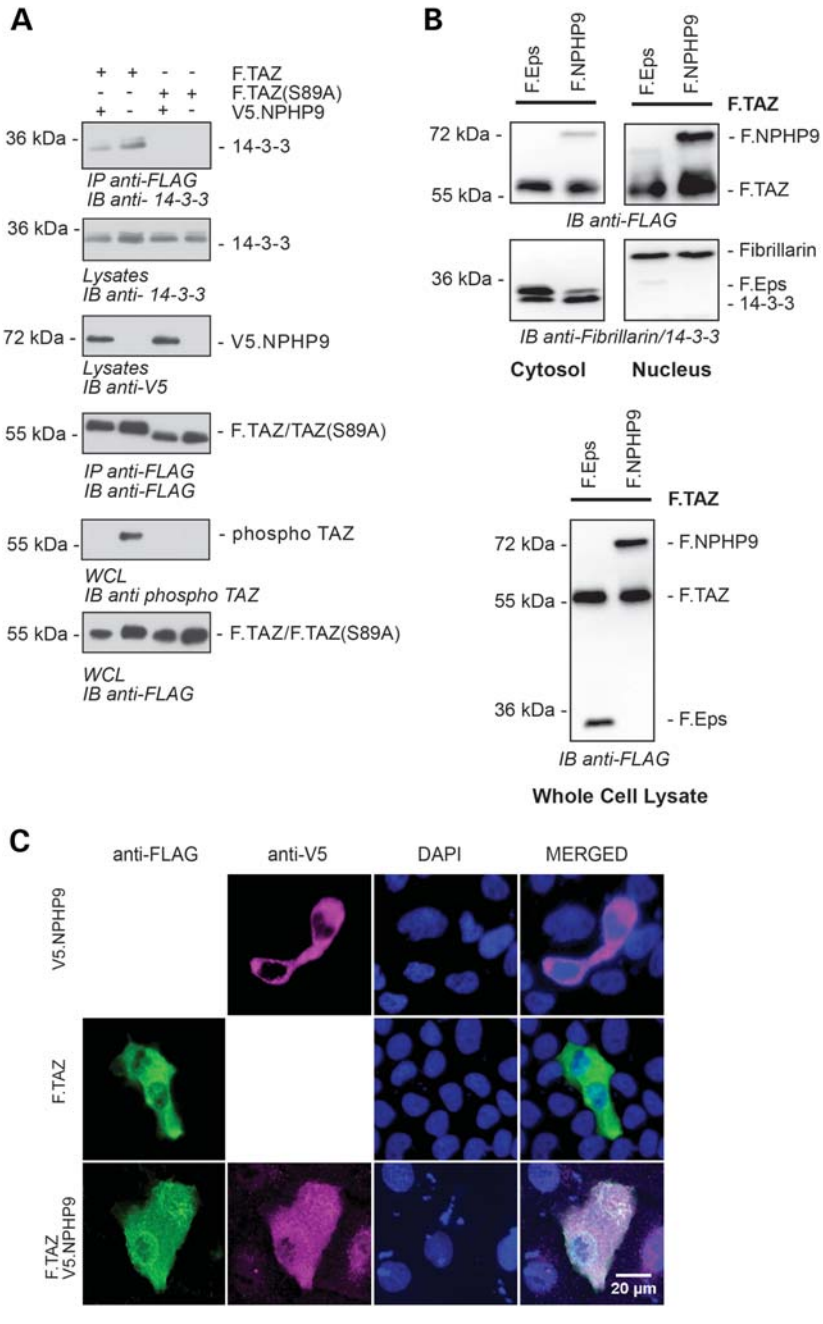

Figure 2. In the presence of NPHP9, TAZ is preferentially located in the nucleus. (**A**) HEK293T cells were transiently transfected with the constructs indicated. FLAG.TAZ was immunoprecipitated in the presence or absence of V5.NPHP9, and co-precipitating 14-3-3 protein was detected by immunoblotting. TAZ carrying a mutant 14-3-3 binding motif (S89A) served as negative control. Co-expression of NPHP9 abolished the interaction of TAZ with 14-3-3 and accordingly resulted in a marked decrease of TAZ phosphorylated at S89. This indicates that TAZ is no longer bound to the cytoplasmic adaptor protein 14-3-3 and might be shifted to the nucleus. (**B**) HEK293T cells were transiently transfected with the constructs indicated and subjected to cell fractionation experiments. Co-expression of NPHP9 leads to a marked increase of TAZ in the nuclear fraction in comparison with a control protein (Eps). NPHP9 itself was also abundantly found in the nuclear fraction. Fibrillarin and 14-3-3 were used as nuclear and cytosolic marker proteins, respectively. (**C**) MCF-10A breast epithelial cells were co-transfected with FLAG-tagged TAZ and V5-tagged NPHP9. Immunofluorescence analysis was used to determine the subcellular localization of transfected TAZ and NPHP9. When expressing NPHP9 alone, it was exclusively localized to the cytoplasm, while in the presence of TAZ, NPHP9 was also present in the nuclei. The transfection of TAZ alone showed a predominant but not exclusive cytoplasmatic staining; however, in cells with NPHP9 and TAZ co-expressed, TAZ was shifted to the nuclei.

epithelial cells (MCF10A). TAZ and NPHP9 showed a predominant cytoplasmic localization when transfected alone (Fig. 2C). However, co-expression induced a nuclear translocation of both proteins, suggesting that NPHP9 caused the co-delivery of TAZ and NPHP9 into the nucleus.

NPHP9 and TAZ interact, and mutation of the 14-3-3 binding motif enhances binding

We next tested whether NPHP9 and TAZ interact, which might be a prerequisite for nuclear translocation. Both proteins

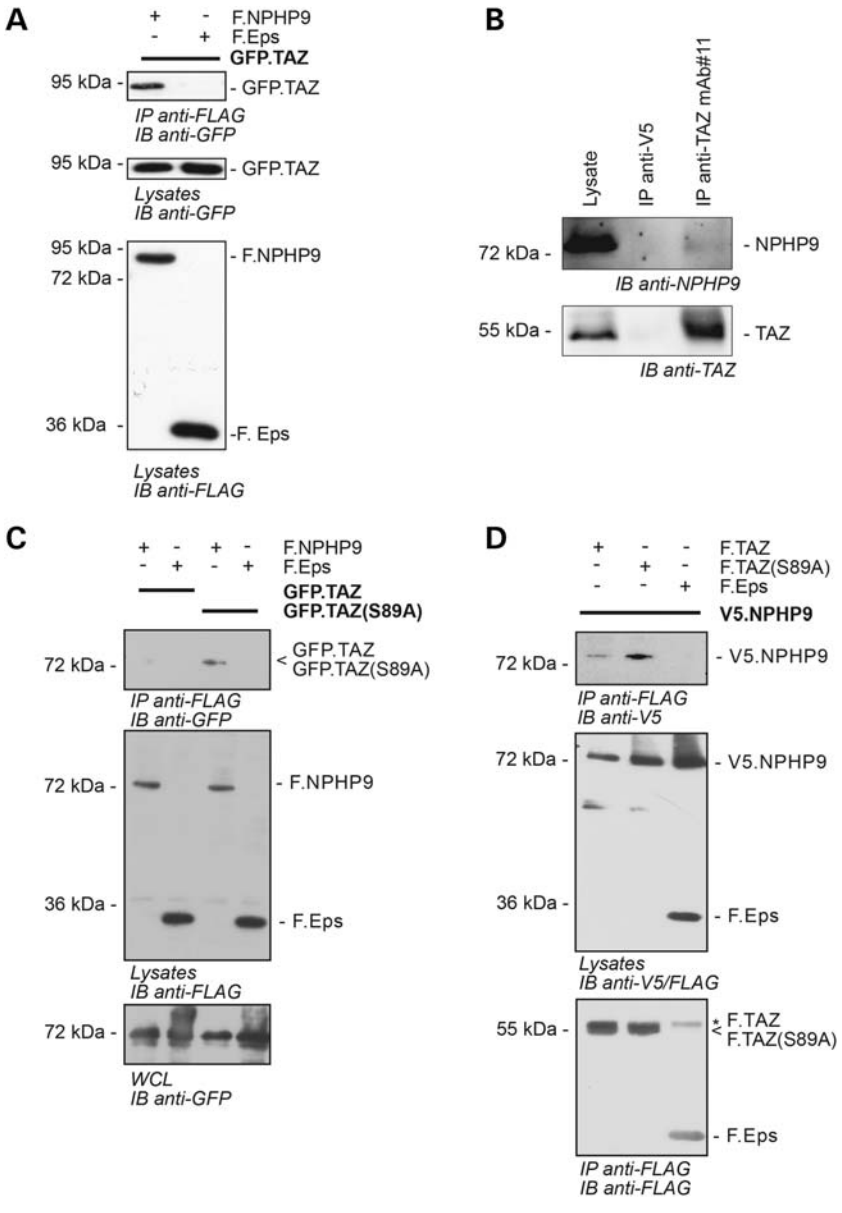

Figure 3. NPHP9 preferentially interacts with unphosphorylated/nuclear TAZ. (**A**) After the transfection of the indicated plasmids into HEK293T cells and immunoprecipitation of NPHP9 or a control protein (Eps) with FLAG beads, western blot analysis revealed that GFP.TAZ co-precipitates with NPHP9. (**B**) Murine lung tissue was homogenized, and TAZ was immunoprecipitated from the resulting protein lysates using a specific monoclonal TAZ antibody or a control antibody and Protein G beads. NPHP9 could be detected in the precipitates of TAZ, but not in the negative control (upper panel). Anti-TAZ staining revealed the efficient precipitation of TAZ (lower panel). (**C**) In the experimental setting of (A), GFP.TAZ-S89A was added. GFP.TAZ-S89A contains the mutant TAZ lacking the 14-3-3 binding motif and thus being considered as 'nuclear' TAZ. Western blot analysis after the immunoprecipitation of NPHP9 or a control protein revealed that F.NPHP9 interacts stronger with TAZ S89A compared with wild-type. (**D**) To confirm these data, the immnunoprecipitation experiment was done vice versa pulling down F.TAZ, F.TAZ-S89A and a control protein (Eps). When pulling down F.TAZ-S89A, more V5.NPHP9 co-precipitated in comparison with F.TAZ wild-type, confirming that TAZ-S89As more likely to interact with NPHP9 either due to the same nuclear localization or due to a stronger affinity of TAZ-S89A to NPHP9 (the asterisk marks the heavy chain of the antibodies).

were expressed and subjected to co-immunoprecipitation experiments. Interestingly, GFP-tagged TAZ strongly co-precipitated with FLAG.NPHP9 (Fig. 3A). To confirm that this interaction occurs between the endogenous proteins as well, we generated monoclonal antibodies directed against full-length murine TAZ. Specificity of the clone used in this study was demonstrated using lysates of transfected 293T cells (Supplementary Material, Fig. S3). Using this antibody for immunoprecipitation out of protein lysates from murine lung, we were able to detect co-precipitating NEK8 with an NEK8-specific antiserum (Fig. 3B). The hippo pathway controls TAZ nuclear delivery through the phosphorylation of TAZ and 14-3-3-mediated retention in the cytoplasm. To test whether 14-3-3-dependent retention may interfere

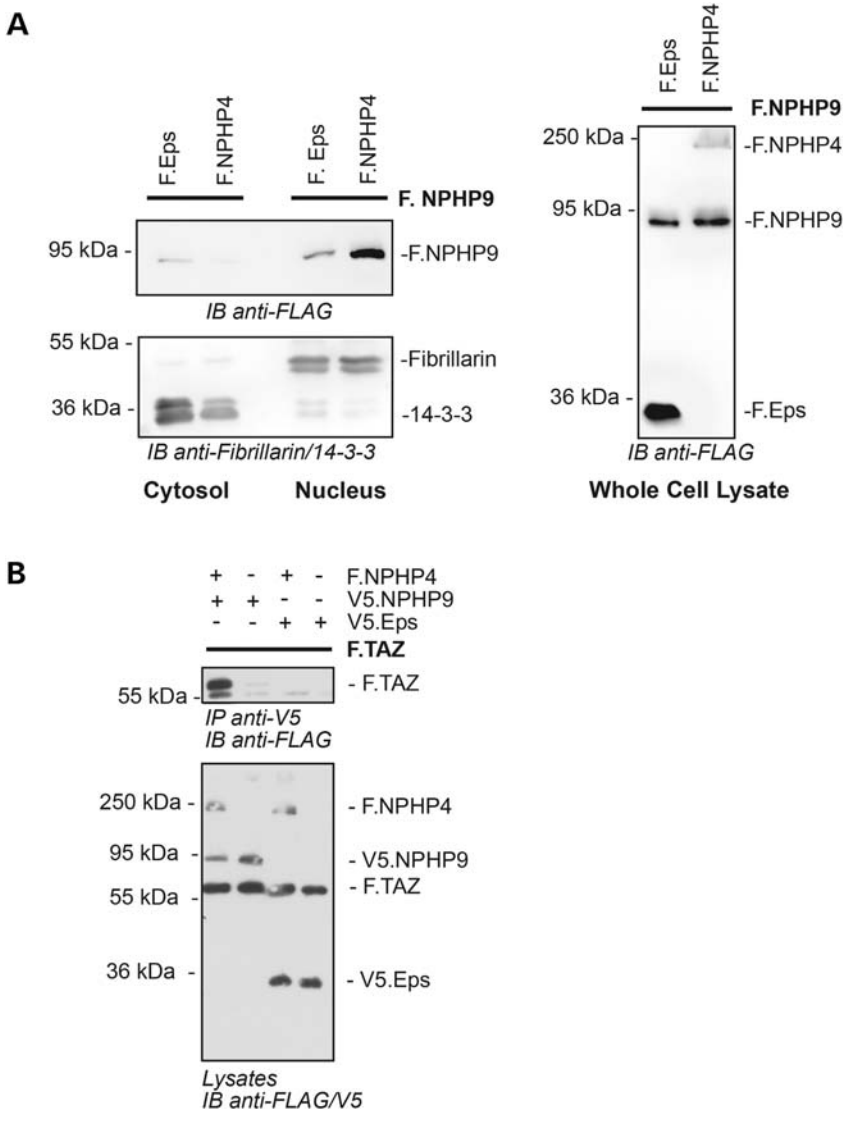

Figure 4. NPHP4, a known modulator of the hippo pathway, translocates NPHP9 to the nucleus and enhances the physical NPHP9–TAZ interaction. (**A**) HEK293T cells were transfected with the constructs indicated to perform cell fractionation experiments. Co-expression of NPHP4 increases the abundance of NPHP9 in the nucleus in comparison with a control protein (Eps). Fibrillarin and 14-3-3 were used as nuclear and cytosolic marker proteins, respectively. (**B**) Lysates from HEK293T cells expressing the indicated constructs were subjected to immunoprecipitation using a rabbit anti-V5 antibody. Western blot analysis reveals that the co-expression of NPHP4 clearly enhances the interaction of NPHP9 with TAZ.

with NPHP9 interaction and nuclear delivery, we expressed wild-type TAZ as well as a mutant version (S89A) that cannot be phosphorylated and does not interact with 14-3-3 (22). Consistent with the described role of NPHP9 in mediating nuclear translocation of TAZ, TAZ-S89A showed a significantly stronger interaction with NPHP9 in the co-expression experiments (Fig. 3 C and D). Although this finding could, in principle, be explained by enhanced co-localization of TAZ-S89A and NPHP9 in the nucleus and co-precipitation from nuclear lysate, it is important to note that nuclei had been removed prior to performing the co-immunoprecipitation experiments. These data suggested that 14-3-3 and NPHP9 may compete for TAZ binding, with 14-3-3 favouring cytoplasmic retention and NPHP9 mediating nuclear delivery.

NPHP4 regulates NPHP9 localization

We have recently shown that NPHP4 interacts with the serine–threonine kinase Lats to inhibit TAZ phosphorylation at the 14-3-3 binding site, resulting in TAZ transcriptional activity. We therefore hypothesized that NPHP4 may promote NPHP9/TAZ interaction and nuclear delivery of the tandem protein complex similar to the scenario where we mutated the 14-3-3 binding site of TAZ. To test this hypothesis, we performed cell fractionation and co-immunoprecipitation experiments. When analysing the subcellular localization of NPHP9, we found that NPHP4 was a potent inducer of NPHP9 nuclear translocation without affecting overall NPHP9 protein levels (Fig. 4A). Thus, NPHP4 not only promotes the nuclear accumulation of TAZ [as described before (4)] but also induces a

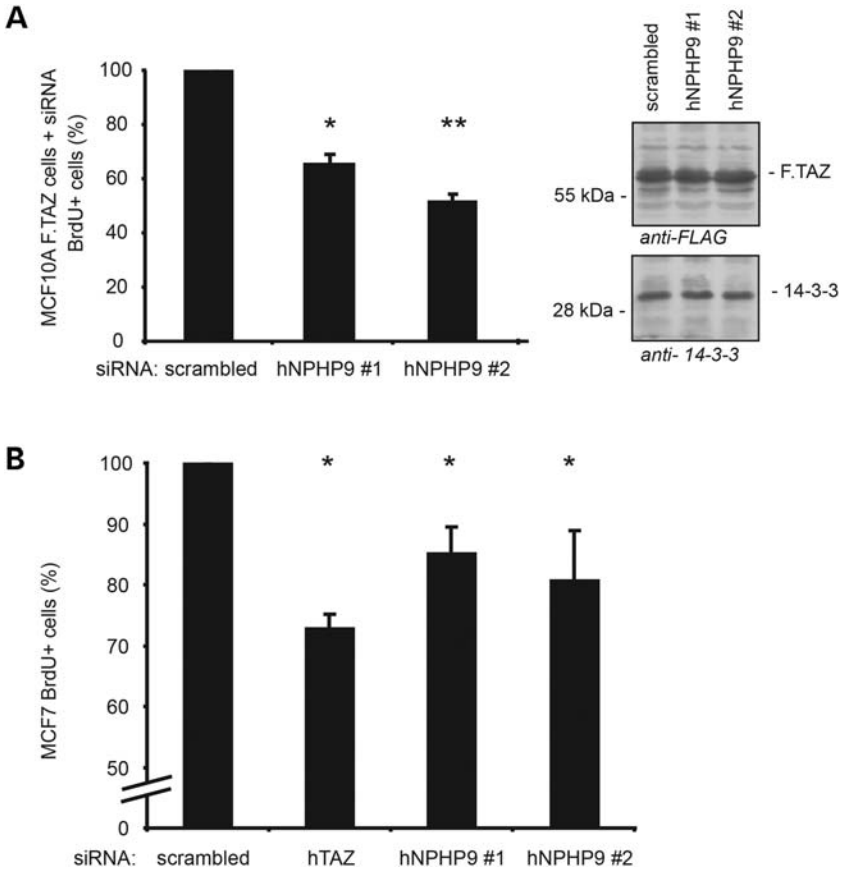

Figure 5. Knockdown of NPHP9 results in reduced proliferation rate in MCF7 cells and dramatically reverses TAZ-induced hyperproliferation in stable TAZ-overexpressing cells. (**A**) MCF10A cells overexpressing F.TAZ were transfected with the indicated siRNAs and were labelled with BrdU for 3 h. Afterwards, the cells were stained with an anti-BrdU antibody and analysed by FACS. MCF10A cells overexpressing TAZ show a dramatic increase in proliferation as shown in Supplementary Material, Fig. S2. The knockdown of NPHP9 in these cells results in a marked decreases of the hyperproliferation induced by TAZ overexpression. (**B**) MCF-7 cells were transfected with the siRNAs indicated. Forty-eight hours after transfection, the cells were labelled with BrdU for 3 h, stained with an anti-BrdU antibody and analysed by FACS. As expected and previously described, the knockdown of TAZ led to reduced cell proliferation, which was also seen after the knockdown of NPHP9 in the same experiment ($n = 3$; $^*P < 0.05$ compared with the negative control; error bars represent SEM; the proliferation rate of the cells treated with scrambled control siRNA was set to 100%).

marked shift of NPHP9 to the nucleus, which is consistent with our hypothesis. Consequently, we assumed that NPHP4 might also be able to enhance the interaction of TAZ and NPHP9 in the nucleus. Accordingly, we performed TAZ–NPHP9 co-precipitation experiments in the presence and absence of NPHP4. Further supporting our model, co-expression of NPHP4 dramatically increased the amount of co-precipitating TAZ when pulling down NPHP9 (Fig. 4B). Taken together, these data suggested that NPHP4, by inhibiting TAZ phosphorylation at the 14-3-3 binding site, leads to the tandem nuclear accumulation of TAZ and NPHP9.

Knockdown of NPHP9 ameliorates TAZ-induced hyperproliferation

Since TAZ is a potent regulator of cell proliferation and tumorigenesis *in vivo* (10), we next explored the effect of NPHP9 in this setting. It has been shown previously that overexpression of TAZ in the non-transformed breast epithelial cell line MCF10A leads to an increase in proliferation (11). Using lentiviral gene transfer, we expressed FLAG.TAZ in MCF10A cells. The empty lentiviral vector was used for a control. BrdU staining and FACS analyses confirmed the expected strong increase in proliferation in the TAZ-expressing cells (Supplementary Material, Fig. S4A). To analyse the impact of NPHP9 on the proliferative potential in these cells, we used two different NPHP9-targeting siRNAs for RNA interference-mediated knockdown experiments (Supplementary Material, Fig. S4B). Interestingly, knockdown of NPHP9 led to a significant reduction in TAZ-induced cell proliferation (Fig. 5A), suggesting that NPHP9 and TAZ act in a common pathway. Consistent with these data, knockdown of TAZ and NPHP9 in the transformed breast cancer cell line MCF-7 led to a similar reduction of BrdU incorporation (Fig. 5B). This could be confirmed in MDA-MB-231 cells, another breast cancer cell line (Supplementary Material, Fig. S5). Taken together, these data indicated that NPHP9 and TAZ control the proliferation rate of hippo-responsive cancer cells.

DISCUSSION

NPH comprises a very heterogeneous group of paediatric polycystic kidney diseases that show phenotypic overlaps with other genetic syndromes, such as Joubert, Bardet–

Biedel, Senior–Loken and many other syndromes. Like all of these syndromes, NPH is caused by the mutation of genes encoding for ciliary proteins. Extensive research efforts over the last decade on the function of the encoded proteins identified several pathways to be controlled by primary cilia, e.g. WNT signalling (23), the Shh pathway (24) or mTOR signalling (25). Recently, we identified NPHP4 as an inhibitor of the hippo signalling cascade (5). This pathway plays an important role in the regulation of cell proliferation, apoptosis and tumorigenesis (8). Whether hippo signalling is linked to ciliary biology and function is still elusive. We could previously demonstrate that the ciliary protein NPHP4, by interacting with the central kinase LATS, inhibits the phosphorylation of YAP and TAZ, thus leading to the activation of TAZ/YAP/TEAD-dependent pro-proliferative transcriptional activity. Loss of NPHP4 in patients would therefore result in reduced proliferation rates that could explain the overt degenerative phenotype displayed in the majority of NPH kidneys. Happe *et al.* (26) recently described high levels of the hippo downstream effector YAP in the cyst-lining epithelium in mouse models with autosomal-dominant polycystic kidney disease (ADPKD) and in renal biopsies of ADPKD patients. ADPKD is characterized by the development of cystic kidneys with a highly enlarged organ volume and a clear proliferative aspect. We therefore assumed that the balance of hippo signalling and TAZ/YAP activity might be critical for the development and maintenance of the renal architecture. Shifting this balance towards high-TAZ/YAP activity might occur in proliferative diseases with increased organ size such as ADPKD, whereas low hippo effector activity would be associated with degenerative phenotypes typically observed in NPH.

Following the identification of NPHP4 as an inhibitor of hippo signalling, we have now identified a second component of the NPHP complex, NPHP9, to influence hippo signalling in the same direction but by a clearly distinct mechanism. In contrast to NPHP4 exerting the effect on TAZ via the inhibition of the Lats kinase, we show that NPHP9 acts more downstream in the hippo pathway, directly stabilizing TAZ in the nucleus. Obviously, the NPH proteins can alter hippo signalling on different levels pointing to a close interplay between hippo signalling and NPH proteins: whereas NPHP4 inhibits the Lats-induced phosphorylation of TAZ, NPHP9 preferentially binds to this non-phosphorylated TAZ and enhances nuclear delivery of TAZ. Therefore, NPHP4 acts upstream of NPHP9 and promotes nuclear localization of the NPHP9/TAZ complex (Fig. 6). Strikingly and in contrast to wild-type NPHP9, the three known patient mutations failed to activate TAZ/TEAD transcription in our HEK293T cell-based model, providing first evidence that disease-causing mutations affect hippo signalling. Very recently, it has been reported that these patient mutations do not affect the kinase activity of NPHP9 (21), suggesting that the kinase activity does not play a causative role in the pathophysiology of NPH. Regarding hippo signalling, this was confirmed by our data: kinase-dead NPHP9 had exactly the same effect on TAZ/TEAD activation as wild-type NPHP9. Taken together, our study supports the concept that the loss of inhibition of hippo signalling and thereby the lacking activation of TAZ could be a central disease mechanism in NPH.

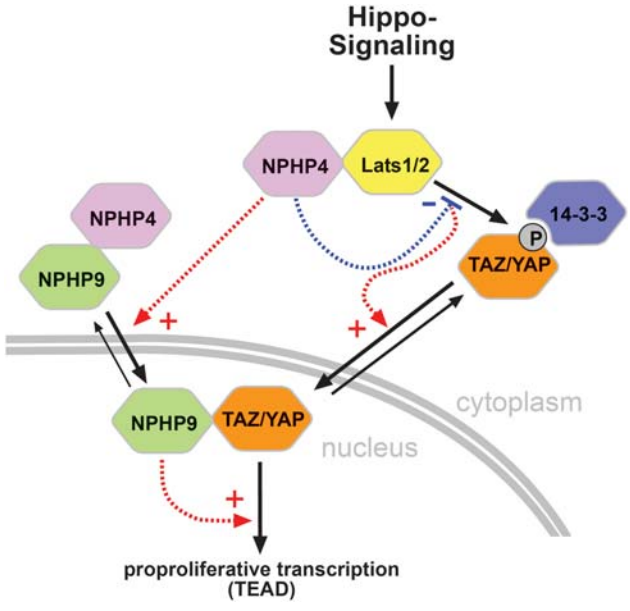

Figure 6. Schematic model of NPHP4 and NPHP9 as activators of TAZ/TEAD transcription. NPHP4 interacts with LATS, thereby inhibiting LATS-dependent phosphorylation of TAZ at the 14-3-3 binding motif at serine-89 (5). Non-phosphorylated TAZ translocates to the nucleus, where it activates TEAD-dependent transcription. In addition to its effects on LATS and TAZ, NPHP4 induces nuclear translocation of NPHP9, which preferentially binds nuclear TAZ, thereby further increasing TAZ/TEAD activity.

In addition, our study provides evidence for a new paradigm of NPH protein function. To date, NPH proteins have been described to form one or more protein complexes located at the base of primary cilia, at the centrosome (2,3) and at the nuclear envelope (27). The fact that NPHP4 acts upstream of NPHP9 gives rise to the hypothesis that NPHP proteins not only form a protein complex of equal players, but also might build up an NPH signalling cascade. This concept of a signalling hierarchy is supported by our previous study on the regulation of Pyk2-induced tyrosine phosphorylation of NPHP1 through NPHP4 (28) and was further confirmed by recent studies that identified NPHP9 to be anchored in the ciliary compartment through NPHP2 (29) and to act downstream of NPHP2 in a zebra fish model (30). Our data revealed that NPHP9 is an effector protein of NPHP4 in terms of hippo signalling. Previous studies have demonstrated that another NIMA-related kinase, NEK1 shuttles through the nuclear compartment (31). NPHP9/NEK8 is localized in primary cilia (29) and associated with ciliogenesis (21) and is therefore a candidate for a messenger signalling molecule shuttling back and forth between the ciliary and the nuclear compartment. Further studies will have to address the exact ciliary and nuclear functions of NPHP9 as downstream effector of NPH protein complexes and inhibitor of hippo signalling.

The finding that NPHP4 and NPHP9 act together in a common pathway that ultimately activates the downstream hippo effectors TAZ and YAP and promotes proliferation has another important implication beyond the pathogenesis of hereditary ciliopathies and cystic kidney diseases. The NPHP4–NPHP9 signalling axis described in this study might be an important regulator of growth and proliferation

in tumour cells as implicated by our knockdown data (Fig. 5). Therefore, it might present a potential target in numerous types of tumours with high levels of active TAZ and YAP. Whereas to our knowledge NPHP4 has not been linked to cancer, NPHP9 was found to be upregulated in a subset of human breast cancer samples (18). Interestingly, two other members of the NPH protein complex that had been associated with cancer before (19,20) show different effects on hippo signalling than NPHP4 and NPHP9, suggesting a complex and differential regulation mediated by NPHP proteins. TAZ has been described as an oncogene, and TAZ overexpression was found in most breast cancer cell lines and several invasive breast cancer tissues (11). However, the phosphorylation status of TAZ in these cancer samples has not been studied yet. This phosphorylation status can be influenced by NPHP9, and the reported overexpression of NPHP9 in breast cancer might result in an activation of TAZ even without affecting total expression levels of TAZ. Further studies on localization and phosphorylation of TAZ are needed to gain a better understanding of the impact of NPHP9 in tumorigenesis.

MATERIALS AND METHODS

Cell culture

HEK293T (human embryonic kidney cell line 293T), MDA-MB-231 and MCF-7 breast cancer cell lines were maintained in DMEM (Dulbecco's modified Eagle's medium) supplemented with 10% FBS (fetal bovine serum). MCF10A cells were cultured in DMEM/F12 supplemented with 5% horse serum, 0.5 μg/ml hydrocortisone, 100 ng/ml cholera toxin, 20 ng/ml EGF and 10 μg/ml insulin as previously described (32).

Cell fractioning

HEK293T cells were transiently transfected with the indicated constructs, using the calcium phosphate method. Cells were disrupted in a hypotonic buffer (10 mM HEPES, pH 7.9, 1.5 mM $MgCl_2$ 10 mM KCl, 0.5 mM DTT, 0.05% NP40, protease inhibitors). After centrifugation at 3000*g* for 10 min, the cytoplasmic fraction was taken from the supernatant. The pellet was washed with PBS and, at 10 000*g*, treated with a hypertonic buffer (5 mM HEPES, pH 7.9, 1.5 mM $MgCl_2$, 0.2 mM EDTA, 0.5 mM DTT, 26% glycerol, 300 mM NaCl, protease inhibitors) after centrifugation for 10 min to yield the nuclear fraction. Both fractions were analysed by western blot.

Immunofluorescence

MCF10A cells were seeded onto coverslips and transfected with the indicated plasmids, using Genejuice (Novagen) transfection reagent (5). Twenty-four hours after transfection, cells were rinsed with PBS several times and fixed with 4% PFA for 10 min. After blocking with 5% normal donkey serum and 0.1% Triton X-100 in dPBS, cells were sequentially stained with the indicated antibodies [primary antibodies: rabbit anti-FLAG (pAB), mouse anti-V5 (mAB); secondary antibodies: Cy3-conjugated anti-rabbit-IgG and Cy2-conjugated anti-mouse-IgG from Jackson ImmunoResearch]. Afterwards, the coverslips were mounted with Prolong Gold (Invitrogen) and subjected to immunofluorescence microscopy. Pictures were taken with an Axiovert 200 microscope (objective: C-Apochromat 63×/1.22 W) equipped with an Axiocam MRm and the Apotome system (Carl Zeiss MicroImaging, Jena, Germany) using Axiovision 4.8 for acquisition and subsequent image processing (Carl Zeiss MicroImaging). Figures were assembled using Macromedia Freehand 11 (Adobe).

Luciferase assays

The luciferase reporter plasmid (pGBD-Hyg-Luc) was transfected together with an activator plasmid (pGal4-TEAD) and the indicated expression plasmids (TAZ, YAP, NPHP4, NPHP9; control: empty pcDNA6) into HEK293T cells in a 96-well format, using LipofectamineLTX (Invitrogen) as described previously (5). The total amount of DNA was always adjusted with empty pcDNA6. Renilla encoded by pGL 4.74 (Promega) was used for normalization. Renilla luciferase and firefly luciferase activities were measured by using a dual-luciferase reporter assay system (Promega) in a luminometer (Mithras LB940, Berthold) 24 h after transfection. Transfections and measurements were done in triplicate for each single experiment and each experiment was repeated at least three times. Error bars shown in the figures represent SEM (standard error of the mean). Equal expression of the transfected proteins was confirmed by western blot analysis.

Co-immunoprecipitation

HEK293T cells were transiently transfected using the calcium phosphate method, and co-immunoprecipitation was performed as described previously (33). Briefly, the day after transfection, cells were harvested with ice-cold PBS. A small aliquot of this cell suspension was taken, and the cells were lysed directly in SDS–PAGE sample buffer (WCL). The remaining cells were lysed in a 1% Triton X-100 buffer [1% Triton X-100, 20 mM Tris–HCl, pH 7.5, 50 mM NaCl, 50 mM NaF, 15 mM $Na_4P_2O_7$, 2 mM Na_3VO_4 and PIM complete (protease inhibitor mix; Roche)] for 15 min on ice. After centrifugation at 20 000*g* (15 min, 4°C) and ultracentrifugation at 100 000*g* (30 min, 4°C), a small aliquot of each supernatant was preserved and diluted with 2× SDS–PAGE sample buffer for later western blot analysis (i.e. lysate). The remaining supernatants were incubated for 2 h at 4°C with anti-FLAG(M2) antibody covalently coupled to agarose beads (Sigma) or with 1 μg of the appropriate first antibody and 20 μl of protein-G-sepharose beads (GE). The beads were washed extensively with lysis buffer, and bound proteins were resolved by SDS–PAGE, blotted onto PVDF-membranes and visualized with enhanced chemiluminescence after the incubation of the blots with the respective antibodies. Immunoprecipitation with endogenous proteins from murine lungs was performed as previously described for murine kidneys (34). Lungs from five wild-type BL6 mice were homogenized in 3–4 ml of lysis buffer (20 mM Tris–HCl, pH 7.5/1% Triton X-100/25 mM NaF/12.5 mM $Na_4P_2O_7$/0.1 mM EDTA/50 mM NaCl/2 mM Na_3VO_4 and protease inhibitors) using a Wheaton glas-glas homogenizer

(2 ml, 60 strokes) followed by a dounce glas-glas homogenizer (tight pestle, 40 strokes). After centrifugation to remove cellular debris, the supernatant was subjected to an ultracentrifugation (100 000*g*) for 30 min. Immunoprecipitation with control antibody (V5 mAB, Serotec) or anti-TAZ antibody and Prot G beads was performed as described above for cell lysates.

Plasmids, reagents and antibodies

TAZ wild-type and TAZ S89A cDNAs were kindly provided by Michael Yaffe (Massachusetts Institute of Technology, Boston, MA, USA), NPHP8 cDNAs by Ronald Roepman (Radboud University Nijmegen Medical Centre, Nijmegen, The Netherlands) and Gerd Walz (University Hospital of Freiburg, Germany). NPHP9 and NPHP5 were cloned from a human kidney cDNA library. The NPHP9 kinase-dead mutant K33M and the patient point mutations (L330F, H425Y, A497P) were generated afterwards using Quikchange mutagenesis (Stratagene, La Jolla, CA, USA). The GAL4-TEAD reporter system (pGBD-Hyg-Luc; pGal4-TEAD) was purchased from Biomyx (San Diego, CA, USA). Eps, NPHP4 and GFP constructs were described before (28). siRNAs used in knockdown experiments were directed against the following sequences: TAZ: 5′-AGG TACTTCCTCAATCACA-3′ (5,11); scrambled/control: 5′-A AATGTACTGCGCGTGGAGAC-3′; NPHP9#1: 5′-ACGGAC AGTTGGGCACCAATA-3′; NPHP9#2: 5′-CCAGAAGCTGG TGATCATCAA-3′. siRNA strands were purchased from Biomers (Ulm, Germany) or Qiagen.

To generate a stable MCF10A TAZ cell line, TAZ was cloned into a modified pENTR1a vector (Invitrogen) and afterwards recombined into the pLenti6.3/V5 Dest vector, using the GATEWAY system (Invitrogen). After virus production in HEK293T cells, the MCF10A cells were transduced with F9.TAZ pLenti6.3 or vector control, and selection was performed using blasticidin (10 μg/ml).

Antibodies were from Sigma (mouse anti-FLAG/M2 #F3165: western blot 1:10 000, IF1:1000; mouse anti-tubulin #T0198: western blot 1:1.000), Serotec (mouse anti-V5 #MCA1360: western blot 1:5000), Millipore (rabbit anti-V5 AB3792: western blot 1:2000, IF 1:500), Abcam (rabbit anti-fibrillarin #ab5821: western blot 1:500), Santa Cruz (mouse anti-GFP #sc8334: western blot 1:1000; rabbit anti-14-3-3 #sc629: western blot 1:1000), Cell Signaling Technology (rabbit anti-phospho YAP Ser127 #4911: western blot 1:1000; rabbit anti-TAZ/YAP #8418: western blot 1:1000), Genetex (rabbit anti-Nek8/NPHP9 #GTX112027: western blot 1:500).

To generate monoclonal antibodies directed against TAZ, His-tagged murine TAZ full-length (His.mTAZ) was expressed in *Escherichia coli*, affinity-purified and used to immunize mice following a standard immunization protocol (35). Fusions resulted in the generation of more than five specific monoclonal antibodies positively tested in ELISA assays on HIS.TAZ-coated plates. Specificity of selected clones was confirmed by using cell lysates from transfected cells.

qPCR analysis

qPCR analysis was performed as described previously (5). MCF10A cells were transfected with the indicated siRNAs (concentration 20 nM final) using Oligofectamine (Invitrogen). Forty-eight hours after transfection, cells were harvested in Qiazol (Qiagen) and RNA was isolated using the phenol–chloroform method. After DNAse treatment (Ambion), the reverse transcription reaction was performed with ABI's High Capacity cDNA Kit. The efficiency of the NPHP9 siRNAs was confirmed using SYBR Green qPCR (NPHP9 fp: 5′-CTTCTTCACTGCCTGCCTGACT-3′; NPHP9 rp: 5′-GGCCTTTCGCAGGCACAGGT-3′), HPRT1 served as endogenous control (HPRT1 fp: 5′-tgacactggcaaaacaatgca-3′; HPRT1 rp: 5′-ggtccttttcaccagcaagct-3′). All qPCR experiments were performed on the ABI 7900HT System and repeated at least three times. Error bars shown in the figures represent SEM.

BrdU assays

MCF10A, MCF7 or MDA-MB-231 cells were transfected with the indicated siRNAs (concentration 20 nM final) using Oligofectamine (Invitrogen) and processed 48 h after transfection. The cells were labelled with BrdU for 3 h in complete growth medium. Afterwards, the cells were fixed with 70% ethanol overnight, following treatment with 2N HCl/0.5% Triton X-100 and 0.1 M sodium tetraborate. Cells were stained with a mouse anti-BrdU antibody (Sigma) and Alexa 488-conjugated anti-mouse-IgG (Jackson ImmunoResearch). DNA was counterstained with PI (propidium iodide, Sigma) and cells were analysed by FACS as described previously (5). The amount of BrdU+ cells for each condition was calculated in comparison with the scrambled siRNA-treated control cells. Error bars shown in the figure represent SEM.

SUPPLEMENTARY MATERIAL

Supplementary Material is available at *HMG* online.

ACKNOWLEDGEMENTS

We thank Stefanie Keller, Jasmin Manz, Katrin Walter and Ulrike Ackermann for excellent technical assistance and the members of the laboratories for helpful discussions. We thank Mike Yaffe, Ronald Roepman and Gerd Walz for providing cDNAs and antibodies.

Conflict of Interest statement. None declared.

FUNDING

This study was supported by the Deutsche Forschungsgemeinschaft (grants SCHE1562/1 and SFB832 to B.S., SFB832 to T.B., SFB832, SFB829 as well as RE 2246/2-1 to C.R. and BE 3910/4-1 to C.B.), by the Deutsche Nierenstiftung and PKD Foundation to C.B., by the Volkswagen Stiftung (85667 to C.R.) and by Köln Fortune (S.H.).

REFERENCES

1. Benzing, T. and Schermer, B. (2012) Clinical spectrum and pathogenesis of nephronophthisis. *Curr. Opin. Nephrol. Hypertens.*, **21**, 272–278.

2. Hildebrandt, F., Attanasio, M. and Otto, E. (2009) Nephronophthisis: disease mechanisms of a ciliopathy. *J. Am. Soc. Nephrol.*, **20**, 23–35.
3. Sang, L., Miller, J.J., Corbit, K.C., Giles, R.H., Brauer, M.J., Otto, E.A., Baye, L.M., Wen, X., Scales, S.J., Kwong, M. *et al.* (2011) Mapping the NPHP-JBTS-MKS protein network reveals ciliopathy disease genes and pathways. *Cell*, **145**, 513–528.
4. Wolf, M.T. and Hildebrandt, F. (2011) Nephronophthisis. *Pediatr. Nephrol.*, **26**, 181–194.
5. Habbig, S., Bartram, M.P., Muller, R.U., Schwarz, R., Andriopoulos, N., Chen, S., Sagmuller, J.G., Hoehne, M., Burst, V., Liebau, M.C. *et al.* (2011) NPHP4, a cilia-associated protein, negatively regulates the Hippo pathway. *J. Cell Biol.*, **193**, 633–642.
6. Pan, D. (2007) Hippo signaling in organ size control. *Genes Dev.*, **21**, 886–897.
7. Varelas, X. and Wrana, J.L. (2012) Coordinating developmental signaling: novel roles for the Hippo pathway. *Trends Cell Biol.*, **22**, 88–96.
8. Pan, D. (2010) The hippo signaling pathway in development and cancer. *Dev. Cell*, **19**, 491–505.
9. Benhamouche, S., Curto, M., Saotome, I., Gladden, A.B., Liu, C.H., Giovannini, M. and McClatchey, A.I. (2010) Nf2/Merlin controls progenitor homeostasis and tumorigenesis in the liver. *Genes Dev.*, **24**, 1718–1730.
10. Zhou, Z., Hao, Y., Liu, N., Raptis, L., Tsao, M.S. and Yang, X. (2011) TAZ is a novel oncogene in non-small cell lung cancer. *Oncogene*, **30**, 2181–2186.
11. Chan, S.W., Lim, C.J., Guo, K., Ng, C.P., Lee, I., Hunziker, W., Zeng, Q. and Hong, W. (2008) A role for TAZ in migration, invasion, and tumorigenesis of breast cancer cells. *Cancer Res.*, **68**, 2592–2598.
12. Chan, S.W., Lim, C.J., Loo, L.S., Chong, Y.F., Huang, C. and Hong, W. (2009) TEADs mediate nuclear retention of TAZ to promote oncogenic transformation. *J. Biol. Chem.*, **284**, 14347–14358.
13. Cordenonsi, M., Zanconato, F., Azzolin, L., Forcato, M., Rosato, A., Frasson, C., Inui, M., Montagner, M., Parenti, A.R., Poletti, A. *et al.* (2011) The Hippo transducer TAZ confers cancer stem cell-related traits on breast cancer cells. *Cell*, **147**, 759–772.
14. Hossain, Z., Ali, S.M., Ko, H.L., Xu, J., Ng, C.P., Guo, K., Qi, Z., Ponniah, S., Hong, W. and Hunziker, W. (2007) Glomerulocystic kidney disease in mice with a targeted inactivation of Wwtr1. *Proc. Natl Acad. Sci. USA*, **104**, 1631–1636.
15. Tian, Y., Kolb, R., Hong, J.H., Carroll, J., Li, D., You, J., Bronson, R., Yaffe, M.B., Zhou, J. and Benjamin, T. (2007) TAZ promotes PC2 degradation through a SCFbeta-Trcp E3 ligase complex. *Mol. Cell. Biol.*, **27**, 6383–6395.
16. Otto, E.A., Trapp, M.L., Schultheiss, U.T., Helou, J., Quarmby, L.M. and Hildebrandt, F. (2008) NEK8 mutations affect ciliary and centrosomal localization and may cause nephronophthisis. *J. Am. Soc. Nephrol.*, **19**, 587–592.
17. Liu, S., Lu, W., Obara, T., Kuida, S., Lehoczky, J., Dewar, K., Drummond, I.A. and Beier, D.R. (2002) A defect in a novel Nek-family kinase causes cystic kidney disease in the mouse and in zebrafish. *Development*, **129**, 5839–5846.
18. Bowers, A.J. and Boylan, J.F. (2004) Nek8, a NIMA family kinase member, is overexpressed in primary human breast tumors. *Gene*, **328**, 135–142.
19. Lin, Y.W., Yan, M.D., Shih, Y.L. and Hsieh, C.B. (2009) The basal body gene, RPGRIP1L, is a candidate tumour suppressor gene in human hepatocellular carcinoma. *Eur. J. Cancer*, **45**, 2041–2049.
20. Luo, X., He, Q., Huang, Y. and Sheikh, M.S. (2005) Cloning and characterization of a p53 and DNA damage down-regulated gene PIQ that codes for a novel calmodulin-binding IQ motif protein and is up-regulated in gastrointestinal cancers. *Cancer Res.*, **65**, 10725–10733.
21. Zalli, D., Bayliss, R. and Fry, A.M. (2012) The Nek8 protein kinase, mutated in the human cystic kidney disease nephronophthisis, is both activated and degraded during ciliogenesis. *Hum. Mol. Genet.*, **21**, 1155–1171.
22. Kanai, F., Marignani, P.A., Sarbassova, D., Yagi, R., Hall, R.A., Donowitz, M., Hisaminato, A., Fujiwara, T., Ito, Y., Cantley, L.C. *et al.* (2000) TAZ: a novel transcriptional co-activator regulated by interactions with 14–3–3 and PDZ domain proteins. *EMBO J.*, **19**, 6778–6791.
23. Lancaster, M.A. and Gleeson, J.G. (2010) Cystic kidney disease: the role of Wnt signaling. *Trends Mol. Med.*, **16**, 349–360.
24. Goetz, S.C. and Anderson, K.V. (2010) The primary cilium: a signalling centre during vertebrate development. *Nat. Rev. Genet.*, **11**, 331–344.
25. Shillingford, J.M., Murcia, N.S., Larson, C.H., Low, S.H., Hedgepeth, R., Brown, N., Flask, C.A., Novick, A.C., Goldfarb, D.A., Kramer-Zucker, A. *et al.* (2006) The mTOR pathway is regulated by polycystin-1, and its inhibition reverses renal cystogenesis in polycystic kidney disease. *Proc. Natl Acad. Sci. USA*, **103**, 5466–5471.
26. Happe, H., van der Wal, A.M., Leonhard, W.N., Kunnen, S.J., Breuning, M.H., de Heer, E. and Peters, D.J. (2011) Altered Hippo signalling in polycystic kidney disease. *J. Pathol.*, **224**, 133–142.
27. Borgal, L., Habbig, S., Hatzold, J., Liebau, M.C., Dafinger, C., Sacarea, I., Hammerschmidt, M., Benzing, T. and Schermer, B. (2012) The ciliary protein nephrocystin-4 translocates the canonical Wnt regulator Jade-1 to the nucleus to negatively regulate beta-catenin signaling. *J. Biol. Chem.*, **287**, 25370–25380.
28. Liebau, M.C., Hopker, K., Muller, R.U., Schmedding, I., Zank, S., Schairer, B., Fabretti, F., Hohne, M., Bartram, M.P., Dafinger, C. *et al.* (2011) Nephrocystin-4 regulates Pyk2-induced tyrosine phosphorylation of nephrocystin-1 to control targeting to monocilia. *J. Biol. Chem.*, **286**, 14237–14245.
29. Shiba, D., Manning, D.K., Koga, H., Beier, D.R. and Yokoyama, T. (2010) Inv acts as a molecular anchor for Nphp3 and Nek8 in the proximal segment of primary cilia. *Cytoskeleton (Hoboken)*, **67**, 112–119.
30. Fukui, H., Shiba, D., Asakawa, K., Kawakami, K. and Yokoyama, T. (2012) The ciliary protein Nek8/Nphp9 acts downstream of Inv/Nphp2 during pronephros morphogenesis and left-right establishment in zebrafish. *FEBS Lett*, **586**, 2273–2279.
31. Hilton, L.K., White, M.C. and Quarmby, L.M. (2009) The NIMA-related kinase NEK1 cycles through the nucleus. *Biochem. Biophys. Res. Commun.*, **389**, 52–56.
32. Debnath, J., Walker, S.J. and Brugge, J.S. (2003) Akt activation disrupts mammary acinar architecture and enhances proliferation in an mTOR-dependent manner. *J. Cell Biol.*, **163**, 315–326.
33. Dafinger, C., Liebau, M.C., Elsayed, S.M., Hellenbroich, Y., Boltshauser, E., Korenke, G.C., Fabretti, F., Janecke, A.R., Ebermann, I., Nurnberg, G. *et al.* (2011) Mutations in KIF7 link Joubert syndrome with Sonic Hedgehog signaling and microtubule dynamics. *J. Clin. Invest.*, **121**, 2662–2667.
34. Schermer, B., Hopker, K., Omran, H., Ghenoiu, C., Fliegauf, M., Fekete, A., Horvath, J., Kottgen, M., Hackl, M., Zschiedrich, S. *et al.* (2005) Phosphorylation by casein kinase 2 induces PACS-1 binding of nephrocystin and targeting to cilia. *EMBO J.*, **24**, 4415–4424.
35. Kohler, G. and Milstein, C. (1975) Continuous cultures of fused cells secreting antibody of predefined specificity. *Nature*, **256**, 495–497.